SPANDIDOS PUBLICATIONS

ONCOLOGY LETTERS 1: 771-775, 2010

$[Gd@C_{82}(OH)_{22}]_n$ nanoparticles inhibit the migration and adhesion of glioblastoma cells

JING WANG[1*], FENG GU[1*], TING DING[1], XIAOLI LIU[2], GENGMEI XING[2], YULIANG ZHAO[2], NING ZHANG[1] and YONGJIE MA[1]

[1]Central Laboratory of the Oncology Department, Tianjin Medical University Cancer Institute and Hospital, Tianjin 300060; [2]Laboratory for Bio-Environmental Health Science of Nanoscale Materials and Key Laboratory of Nuclear Analytical Technique, Institute of High Energy Physics, Chinese Academy of Sciences, Beijing 100049, P.R. China

Received April 9, 2010; Accepted May 28, 2010

DOI: 10.3892/ol_00000135

Abstract. In our previous study, $[Gd@C_{82}(OH)_{22}]_n$, a fullerene-based nanoparticle, exhibited potent anti-tumor effects in mouse tumor-bearing models without detectable toxicity. The mechanism involved in the anti-tumor effect exerted by $[Gd@C_{82}(OH)_{22}]_n$ remains to be elucidated. This study found that glioblastoma cells treated with $[Gd@C_{82}(OH)_{22}]_n$ nanoparticles showed a significant impairment in migration and adhesion by cell chemotaxis, scratch and adhesion assays *in vitro*. Furthermore, our data showed that the key proteins, CD40 and ICAM-1, were involved in the inhibition of adhesion in the $[Gd@C_{82}(OH)_{22}]_n$ nanoparticle-treated glioblastoma cells. Thus, our study suggests that the $[Gd@C_{82}(OH)_{22}]_n$ nanoparticle is a new potential anti-tumor effector and a therapeutic component for malignant glioblastoma infiltration.

Introduction

Fullerene, the third allotrope of carbon, was synthesized in 1985 (1). Due to its unique geometric structure and chemical properties, fullerene derivatives have attracted interest in physics, chemical, biological and medical applications (2). The endohedral metallofullerenes recently attracted attention due to their special biomedical effect (3,4). Gadolinium fullerene compounds, $Gd@C_{82}$, composed of a Gd^{3+} ion trapped in an 82-carbon fullerene cage, were initially used as a contrast agent in magnetic resonance imaging (MRI) for intracellular labeling and T1 enhancement (5). Based on this structure, $Gd@C_{82}(OH)x$ was studied as a new generation of high-efficiency MRI contrast agents (6,7).

During an investigation using mouse models to compare the anti-tumor efficacy of metallofullerenol nanoparticles with the anti-tumor effects of anti-neoplastic agents CTX (cyclophosphamide) and CDDP (cisplatin), $Gd@C_{82}(OH)_{22}$ (22-nm nanoparticles through large molecular interactions in aqueous solutions) was identified and showed a strong anti-tumor activity (4). This high anti-tumor efficacy was not due to direct toxic effects on tumor cells, and the content of this nanoparticle was less than 0.05% of the exposed dose (4). It was therefore suggested that $[Gd@C_{82}(OH)_{22}]_n$ plays a role by inhibiting the migration and/or adhesion ability of glioblastoma cells.

The present study examined the hypothesis that $[Gd@C_{82}(OH)_{22}]_n$ nanoparticles directly participate in glioblastoma cell migration and adhesion. Cells treated with $[Gd@C_{82}(OH)_{22}]_n$ nanoparticles exhibited significant impairment in a series of migration and adhesion assays *in vitro*. Furthermore, our data showed that the key proteins, CD40 and ICAM-1, were involved in the $[Gd@C_{82}(OH)_{22}]_n$ nanoparticle-mediated adhesion of glioblastoma cells. Results indicated that $[Gd@C_{82}(OH)_{22}]_n$ inhibited cancer cell adhesion through the down-regulation of CD40 and ICAM-1. Thus, $[Gd@C_{82}(OH)_{22}]_n$ nanoparticle may be a new potential anti-tumor effector and therapeutic component for malignant glioblastoma infiltration.

Materials and methods

Cell culture and reagents. Cells from the human glioblastoma cell line LN-229 were obtained from the American Type Culture Collection (Manassas, VA, USA) and cultured in RPMI-1640 with 10% fetal bovine serum (complete medium). The chemotaxis chambers and membranes were acquired from Neuroprobe (Gaithersburg, MD, USA). The recombinant human epithelial growth factor (EGF) was obtained from R&D Systems (Minneapolis, MN, USA). Fibronectin (0.1%) and MTT were from Sigma (St. Louis, MO, USA). The antibodies against CD40, ICAM-1 and β-actin were acquired from Santa Cruz Biotechnology, Inc. (Santa Cruz, CA, USA).

MTT cell proliferation assay. Cells ($1x10^3$/well) were plated in 96-well plates in 100 μl of complete medium. Following

Correspondence to: Dr Yongjie Ma and Dr Ning Zhang, Central Laboratory of the Oncology Department, Tianjin Medical University Cancer Institute and Hospital, Huanhuxi Road, Tiyuanbei, Hexi, Tianjin 300060, P.R. China
E-mail: yongjiemagu@yahoo.com.cn; zhangning@timu.edu.cn

*Contributed equally

Key words: nanoparticle $[Gd@C_{82}(OH)_{22}]_n$, glioblastoma, migration, adhesion

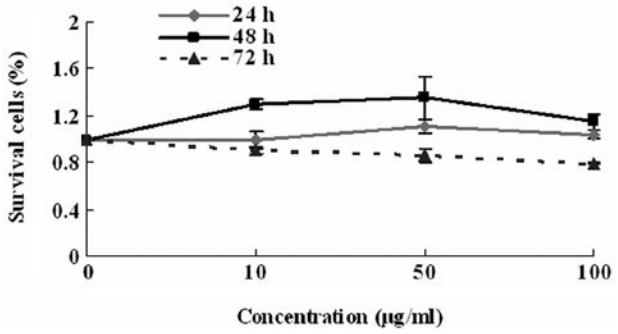

Figure 1. MTT assay of $[Gd@C_{82}(OH)_{22}]_n$ nanoparticle-treated glioblastoma LN-229 cells. A total of 3 doses (10, 50 and 100 μg/ml) of $[Gd@C_{82}(OH)_{22}]_n$ nanoparticles were used. MTT assay was performed after 24, 48 and 72 h of treatment, respectively. The result is representative data from at least three independent experiments. Columns, mean of triplicate measurements.

overnight attachment, the cells were exposed to different concentrations of $[Gd@C_{82}(OH)_{22}]_n$ nanoparticles (10, 50 and 100 μg/ml) for 3 days. To perform the assay, 10 μl of 3-(4,5-dimethylthiazol-2-yl)-2,5-diphenyltetrazolium bromide (MTT) solution was added to each well. After 4 h of incubation at 37˚C, followed by the addition of 150 μl dimethyl sulfoxide to each well and vibration for 10 min, absorbance was measured at 490 nm in a microplate reader. Triplicate wells with pre-determined cell numbers were subjected to the above assay concomitantly with the test samples to normalize the absorbance readings. The experiments were conducted in triplicate and repeated at least three times independently.

Western blotting. Western blotting was performed as described by Zhang *et al* (8). Briefly, the LN-229 cells were serum-starved for 2 h and then treated with $[Gd@C_{82}(OH)_{22}]_n$ nanoparticles for 24 h. The treated and control cells were washed twice with ice-cold phosphate-buffered saline (PBS), and subsequently activated by 10 ng/ml EGF for 0, 5 or 15 min. The reactions were stopped by ice-cold PBS (pH 6.8). The cells were lysed with 1X SDS lysis buffer containing Tris-HCl (pH 6.8), 62.5 mM, 2% SDS and 10% glycerol for 20 min on ice. Samples were boiled for 10 min, followed by centrifugation at 10,000 rpm for 10 min, and supernatants were isolated. Equal amounts of protein were separated by sodium dodecyl sulfate polyacrylamide gel electrophoresis (SDS-PAGE) and electrotransferred onto nitrocellulose membranes (Immobilon-P, Millipore, Billerica, MA, USA). The blots were probed with the appropriate dilutions of primary antibody overnight at 4˚C (CD40, 1:50; ICAM-1, 1:50) and incubated with the proper dilution of alkaline phosphatase-conjugated secondary antibodies.

Chemotaxis assay. Chemotaxis assay was performed as previously described (8). The cells were treated for 2 h in the serum-free medium and then with $[Gd@C_{82}(OH)_{22}]_n$ nanoparticles for 24 h. The cells ($8x10^5$ cells/ml) suspended in binding medium (RPMI-1640, 0.1% BSA and 25 mM HEPES) were added to the upper chambers. The EGF (10 ng/ml) was loaded into the lower chemotaxis chamber. The polycarbonate filter (8-μm pore size; Neuroprobe, Cabin John, MD, USA) was pre-treated with 10 μg/ml fibronectin overnight, air-dried and inserted between the upper and lower chambers. The lower chamber was then incubated at 37˚C in 5% CO_2 for 3.5 h. The filter membrane was rinsed, fixed and stained. The number of migrating cells were counted at a magnification of x400 in three separate fields by light microscopy. The chemotaxis index was determined as the ratio of the number of migrating cells in the nanoparticle gradient to the number of migrating cells in the control medium. For the chemokinesis assay (checkerboard assay), the control and treated cells were suspended in medium containing different concentrations of EGF before being loaded to the upper chambers. Different concentrations of EGF were added to the lower chambers. All of the samples were tested in triplicate, and data are expressed as the mean ± SD. Statistical analysis was carried out to determine the significance of the chemotactic response by using PRISM 3, a two-way analysis of variance analysis.

Scratch assay. The LN-229 cells were plated in 35-mm dishes overnight and starved for 2 h, and subsequently treated with different concentrations (1, 10, 50 and 100 μg/ml) of $[Gd@C_{82}(OH)_{22}]_n$ nanoparticles for 24 h. A scratch was then made with an even trace in the middle of the cells using a 10-μl pipette tip (8). The cells were incubated at 37˚C in 5% CO_2 for an appropriate time period, and the distance of the wound was measured under a light microscope. The samples were tested in triplicate, and the data are expressed as the mean ± SD.

Adhesion assay. The adhesion assay was carried out as previously described (8). The cells were treated for 2 h in the serum-free medium and then with $[Gd@C_{82}(OH)_{22}]_n$ nanoparticles for 24 h. The control or treated cells ($2.7x10^5$/ml) were suspended in complete medium. Then, 1.5 ml cells in the presence of 10 ng/ml EGF were immediately added to a 35-mm dish containing glass coverslips. The coverslips were pre-treated with 10 μg/ml of fibronectin in serum-free medium for 2 h at 37˚C and then air-dried for 30 min at room temperature. After 5, 15 and 30 min of incubation, the cells were gently washed twice with ice-cold PBS and fixed. The cells attached to the coverslips were counted under a light microscope at a magnification of x200.

Statistical analysis. Statistical analysis was carried out using PRISM 3 from GraphPad Software (San Diego, CA, USA). Data are presented as mean ± SD. Statistical significance for comparisons between the groups was determined using Student's paired two-tailed t-test. The results were generated from three independent experiments.

Results

The MTT assay was initially applied to confirm that the $[Gd@C_{82}(OH)_{22}]_n$ nanoparticles had no toxicity towards the LN-229 glioblastoma cells. A total of 3 doses (10, 50 and 100 μg/ml) of $[Gd@C_{82}(OH)_{22}]_n$ nanoparticles were used in this assay. The $[Gd@C_{82}(OH)_{22}]_n$ nanoparticles did not show any cellular toxicity at 24 h (Fig. 1), which was consistent with a previous report by Chen *et al* (4).

Cell migration is a highly dynamic phenomenon that is essential to biological morphogenesis, wound healing, cancer metastasis and immune response (9-12). In order to examine

A

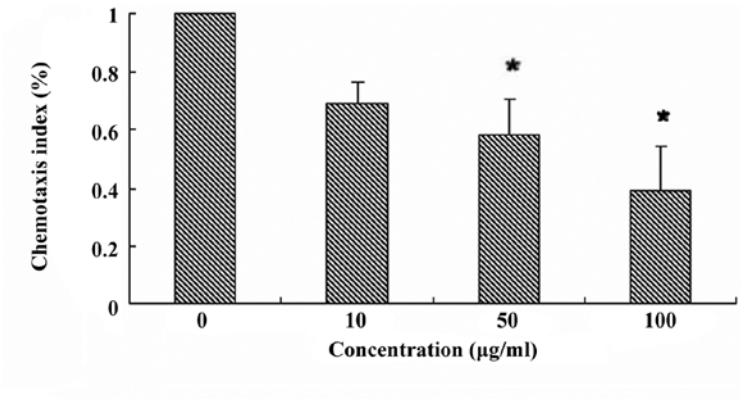

B

EGF (ng/ml)	Upper wells (NP 0 μg/ml)		Upper wells (NP 50 μg/ml)	
Lower wells	0	10	0	10
0	44±7	36±6	36±6	20±4
10	225±27	182±17	158±26	120±8

Figure 2. (A) Chemotaxis and (B) chemokinesis assays of $[Gd@C_{82}(OH)_{22}]_n$ nanoparticle-treated glioblastoma LN-229 cells. A total of 3 doses (10, 50 and 100 μg/ml) of $[Gd@C_{82}(OH)_{22}]_n$ nanoparticles were used in the chemotaxis assay, and 50 μg/ml of $[Gd@C_{82}(OH)_{22}]_n$ nanoparticles (NP) was used in the chemokinesis assay. A 24-h treatment of nanoparticles was performed in the two assays. EGF (10 ng/ml) was used as a chemoattractant (two-way ANOVA analysis, *P<0.05). Columns, mean of triplicate measurements; bars, standard deviation.

A

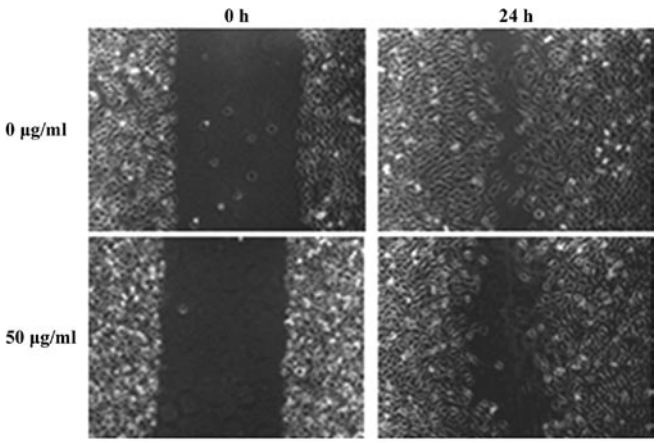

B

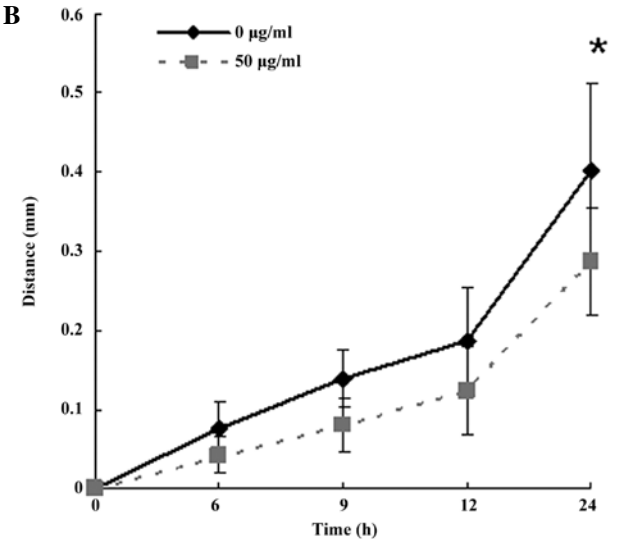

Figure 3. Scratch assay of $[Gd@C_{82}(OH)_{22}]_n$ nanoparticle-treated glioblastoma LN-229 cells. LN-229 cells were treated with 50 μg/ml $[Gd@C_{82}(OH)_{22}]_n$ nanoparticles, and the scratch assay was performed after the 24-h treatment. The migration distance of the cells was measured at various time points (6, 9, 12 and 24 h) after the scratch was made in the culture dish. (A) Images of treated cells at 24 h after the scratch. (B) Migration distance of LN-229 cells at various time points (two-way ANOVA analysis, *P<0.05).

the manner in which $[Gd@C_{82}(OH)_{22}]_n$ nanoparticles affect cell migration, we performed cell chemotaxis and scratch assays. A 48-well EGF-induced chemotaxis model was applied to perform 3 h cell chemotaxis. The cells treated with 50 and 100 μg/ml of $[Gd@C_{82}(OH)_{22}]_n$ nanoparticles showed decreased chemotactic ability compared to the control. The low dose of 10 μg/ml did not show a significant inhibition effect (Fig. 2A). The 50 μg/ml dose of $[Gd@C_{82}(OH)_{22}]_n$ nanoparticles was selected for the experiments mentioned below.

Apart from the chemotaxis assay, we also carried out a chemokinesis assay that presents random cell motility stimulated in a gradient-independent manner (8). Chemokinesis was also impaired in the cells treated with 50 μg/ml of $[Gd@C_{82}(OH)_{22}]_n$ nanoparticles, which may have accounted for the decrease in chemotaxis (Fig. 2B). The change in cell proliferation, however, did not interfere with the chemotaxis of LN-229 cells, as it only took <3 h to complete the chemotaxis assay in this study, shorter than the doubling time.

A scratch assay was used as an *in vitro* assay for wound healing and directional movement (13). When a scratch was created in the fluent monolayer cells, the $[Gd@C_{82}(OH)_{22}]_n$ nanoparticle-treated (50 μg/ml) LN-229 cells required a longer

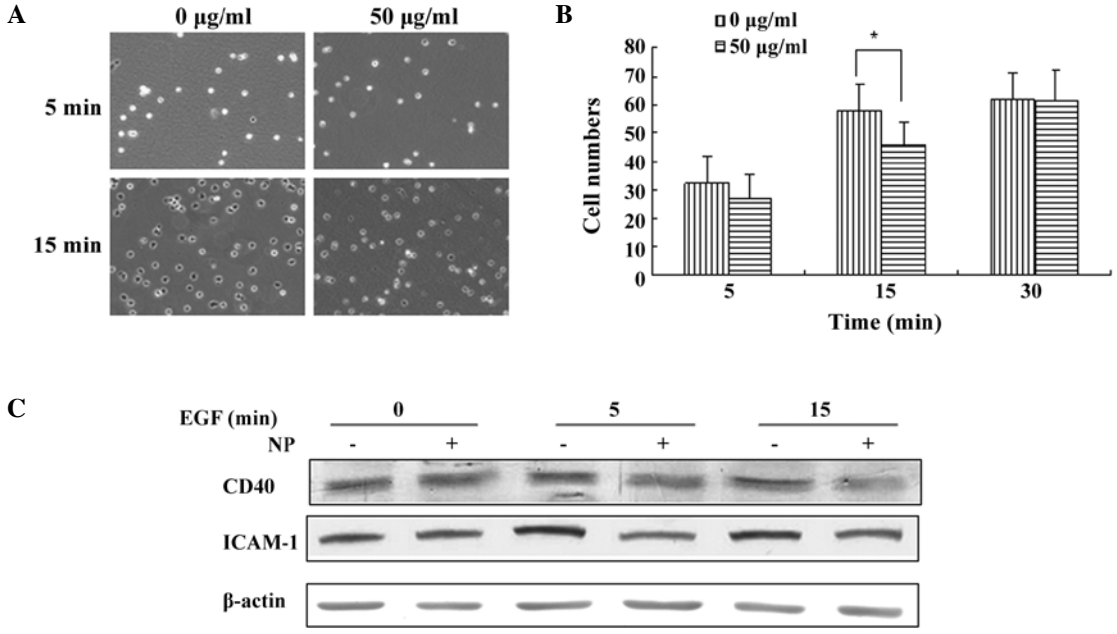

Figure 4. Inhibition of the adhesion ability of $[Gd@C_{82}(OH)_{22}]_n$ nanoparticle-treated glioblastoma LN-229 cells. (A) An adhesion assay was performed after a 24-h treatment in the presence or absence of 50 μg/ml of $[Gd@C_{82}(OH)_{22}]_n$ nanoparticles. Images were captured at 5 and 15 min after the treated cells were loaded in the culture dishes. (B) Quantitative results of the adhesion assay. Data were collected at 5, 15 and 30 min, respectively (two-way ANOVA analysis, $^*P<0.05$). (C) Western blotting of CD40 and ICAM-1 in glioblastoma LN-229 cells. Cell lysates were obtained after a 24-h treatment in the presence or absence of 50 μg/ml of $[Gd@C_{82}(OH)_{22}]_n$ nanoparticles and with 10 ng/ml EGF stimulation for 0, 5 or 15 min, respectively. β-actin was used as a loading control. The results are representative data of at least three independent experiments.

time to fill the gap, further supporting a defect in the migration ability (Fig. 3A and B).

The process of cell movement can be divided into three stages. The first includes the reorganization of the actin work at its leading edge. The second involves adherence to the substrate at the leading edge and the consequent deadherence. The third stage involves the contractile force required by the action of the acto-myosin network to pull the cell forward (14). Therefore, adhesion is critical for cell movement. This study investigated the manner in which $[Gd@C_{82}(OH)_{22}]_n$ nanoparticles affect cell adhesion in LN-229 cells. Following treatment with $[Gd@C_{82}(OH)_{22}]_n$ nanoparticles for 24 h, the adhesion ability of control and treated LN-229 cells were compared. At 5 min of adhesion assay, the adhesion ability of LN-229 cells showed a similar level in the absence or presence of a 50 μg/ml treatment of $[Gd@C_{82}(OH)_{22}]_n$. At 15 min, nanoparticle treatment inhibited the adhesion ability of LN-229 cells (Fig. 4A and B).

CD40, a TNF-R-related cell surface receptor, was reported to be expressed in glioma cells *in vitro* and *in vivo* (15). CD40 up-regulates the expression of ICAM-1 and plays a role in cell adhesion (16,17). The protein level of CD40 and ICAM-1 was detected upon $[Gd@C_{82}(OH)_{22}]_n$ treatment. We found that LN-229 cells treated with 50 μg/ml of $[Gd@C_{82}(OH)_{22}]_n$ nanoparticles exhibited a decreased expression level of CD40 and ICAM-1 responding to a 5- and 15-min EGF stimulation, which was consistent with the decreased adhesion ability.

Discussion

The rapid development of nanotechnology and the discovery of its desirable applications has allowed for a wide variety of nanoparticles to provide a broad range of opportunities in multidisciplinary fields, such as medicine, therapeutics, clinical diagnosis (18), disease treatment and physiological and immunological mechanisms (19). By using novel nanoparticles to identify and treat cancer, nano-medicine has the potential to specifically treat cancer cells while leaving healthy cells intact in the human body (20). Manufactured nanoparticles, such as carbon black and fullerene (the third allotrope of carbon), are widely used due to their desirable properties in the medical field (5). Our previous studies demonstrated that Gadolinium fullerene compounds, $Gd@C_{82}$, composed of a Gd^{3+} ion trapped in an 82-carbon fullerene cage, are able to effectively inhibit tumor growth without detectable cytotoxicity *in vitro* and toxic side effects *in vivo* (2,4,5,21). Based on this function, we hypothesized that $Gd@C_{82}(OH)x$ influences the migration and adhesion of tumor cells.

Directed cell migration and polarity are crucial in various biological processes, including wound healing and immune responses, as well as in pathological phenomena, such as tumor invasion and metastasis (9-12). In the present study, the chemotaxis and scratch assays showed that the $[Gd@C_{82}(OH)_{22}]_n$ nanoparticle-treated LN-229 cells exhibited a significantly decreased migration ability. However, what role the nanoparticle plays in migration remains to be elucidated, and further studies are necessary.

ICAM-1 is one of the critical adhesion proteins of cancer cells and is present constitutively on the cell surface (16,22). The investigation of CD40 and ICAM-1 interaction showed that CD40 activation up-regulates ICAM-1 expression with the concomitant enhanced adhesion of tumor cells, and this process is mediated via the p38 MAPK signal transduction pathway (16). In the present study, glioblastoma cells treated

with $[Gd@C_{82}(OH)_{22}]_n$ nanoparticles exhibited CD40 and ICAM-1 down-regulation followed by decreased adhesive ability. This suggests that the $[Gd@C_{82}(OH)_{22}]_n$ nanoparticle function on cell adhesion is mediated by CD40/ICAM-1 signaling.

We found that the $[Gd@C_{82}(OH)_{22}]_n$ nanoparticle is a type of nano-material that exerts an anti-tumor effect. Our results suggest that $[Gd@C_{82}(OH)_{22}]_n$ nanoparticles, due to their unique physical size and surface chemical properties, can target multiple molecular processes simultaneously and, therefore, are promising for the development of more effective tumor chemotherapy.

Acknowledgements

This study was supported by the China 973 Program (2006CB705600 and 2010CB933900), the 863 Program (2007AA021802), the National Scientific Foundation of China (30700253 and 30800355), and the Tianjin Commission of Science and Technology (2008ZCKFSH04800).

References

1. Kroto HW, Heath JR, O'Brien SC, Curl RF and Smalley RE: C60: Buckminsterfullerene. Nature 318: 162-163, 1985.
2. Wang J, Chen C, Li B, *et al*: Antioxidative function and biodistribution of $[Gd@C_{82}(OH)_{22}]_n$ nanoparticles in tumor-bearing mice. Biochem Pharmacol 71: 872-881, 2006.
3. Cagle DW, Kennel SJ, Mirzadeh S, Alford JM and Wilson LJ: In vivo studies of fullerene-based materials using endohedral metallofullerene radiotracers. Proc Natl Acad Sci USA 96: 5182-5187, 1999.
4. Chen C, Xing G, Wang J, *et al*: Multihydroxylated $[Gd@C_{82}(OH)_{22}]_n$ nanoparticles: antineoplastic activity of high efficiency and low toxicity. Nano Lett 5: 2050-2057, 2005.
5. Anderson SA, Lee KK and Frank JA: Gadolinium-fullerenol as a paramagnetic contrast agent for cellular imaging. Invest Radiol 41: 332-338, 2006.
6. Mikawa M, Kato H, Okumura M, *et al*: Paramagnetic water-soluble metallofullerenes having the highest relaxivity for MRI contrast agents. Bioconjug Chem 12: 510-514, 2001.
7. Bolskar RD, Benedetto AF, Husebo LO, *et al*: First soluble M@C60 derivatives provide enhanced access to metallofullerenes and permit in vivo evaluation of $Gd@C_{60}[C(COOH)_2]10$ as a MRI contrast agent. J Am Chem Soc 125: 5471-5478, 2003.
8. Zhang B, Gu F, She C, *et al*: Reduction of Akt2 inhibits migration and invasion of glioma cells. Int J Cancer 125: 585-595, 2009.
9. Guo H, Gu F, Li W, *et al*: Reduction of protein kinase c zeta inhibits migration and invasion of human glioblastoma cells. J Neurochem 109: 203-213, 2009.
10. Huang J, Chen K, Gong W, Dunlop NM and Wang JM: G-protein coupled chemoattractant receptors and cancer. Front Biosci 13: 3352-3363, 2008.
11. Kurosaka S and Kashina A: Cell biology of embryonic migration. Birth Defects Res C Embryo Today 84: 102-122, 2008.
12. Rorth P: Collective cell migration. Annu Rev Cell Dev Biol 25: 407-429, 2009.
13. Etienne-Manneville S and Hall A: Integrin-mediated activation of Cdc42 controls cell polarity in migrating astrocytes through PKCzeta. Cell 106: 489-498, 2001.
14. Lefranc F, Brotchi J and Kiss R: Possible future issues in the treatment of glioblastomas: special emphasis on cell migration and the resistance of migrating glioblastoma cells to apoptosis. J Clin Oncol 23: 2411-2422, 2005.
15. Wischhusen J, Schneider D, Mittelbronn M, *et al*: Death receptor-mediated apoptosis in human malignant glioma cells: modulation by the CD40/CD40L system. J Neuroimmunol 162: 28-42, 2005.
16. Li H and Nord EP: CD40/CD154 ligation induces mononuclear cell adhesion to human renal proximal tubule cells via increased ICAM-1 expression. Am J Physiol Renal Physiol 289: F145-F153, 2005.
17. Sumimoto S and Mayumi M: [Role of LFA-1/ICAM-1-dependent cell adhesion in CD40-mediated inhibition of anti-IgM antibody-induced B-cell death]. Nippon Rinsho 54: 1779-1783, 1996.
18. Jain KK: Nanotechnology in clinical laboratory diagnostics. Clin Chim Acta 358: 37-54, 2005.
19. Juillerat-Jeanneret L and Schmitt F: Chemical modification of therapeutic drugs or drug vector systems to achieve targeted therapy: looking for the grail. Med Res Rev 27: 574-590, 2007.
20. LaRocque J, Bharali DJ and Mousa SA: Cancer detection and treatment: the role of nanomedicines. Mol Biotechnol 42: 358-366, 2009.
21. Yin JJ, Lao F, Meng J, *et al*: Inhibition of tumor growth by endohedral metallofullerenol nanoparticles optimized as reactive oxygen species scavenger. Mol Pharmacol 74: 1132-1140, 2008.
22. Roebuck KA and Finnegan A: Regulation of intercellular adhesion molecule-1 (CD54) gene expression. J Leukoc Biol 66: 876-888, 1999.